



## **CORROSION OF EPOXY-COATED REBAR IN MARINE BRIDGES - A 30 YEAR PERSPECTIVE**

Alberto A Sagüés and Kingsley Lau  
Dept. of Civil and Environmental Engineering, University of South Florida  
4202 E. Fowler Ave. ENB118  
Tampa, FL 33620

Rodney G. Powers and Richard J. Kessler  
State Materials Office, Florida Dept. of Transportation  
5007 NE 39<sup>th</sup> Ave  
Gainesville, FL 32609

### **ABSTRACT**

The corrosion performance of epoxy-coated rebar (ECR) over a nearly 30 year service period in Florida marine bridges is presented. Severe ECR corrosion was noted earlier in several of those bridges, built with relatively high permeability concrete. Corrosion development took place later in some other structures with less permeable concrete, with instances where the corrosion was associated with preexisting cracks. Corrosion was found to be associated with coating imperfections and coating disbondment. Laboratory experiments and modeling indicated that macrocell coupling with remote cathodes was an aggravating factor. Quantitative damage functions relating the observed deterioration with service time of the affected bridges are presented. A predictive corrosion initiation-propagation model was developed and the model output is compared with the field results to identify suitable parameters for forecasting future rehabilitation needs. The prognosis for future corrosion development is discussed, with attention to corrosion of ECR in otherwise low permeability concrete with preexisting cracks or local deficiencies.

Keywords: epoxy, rebar, concrete, Florida Keys, corrosion, bridges

### **INTRODUCTION**

Epoxy-coated rebar (ECR) has been used in approximately 300 Florida bridges, principally in an attempt to control corrosion of the substructure in the splash-evaporation zone of marine bridges. Starting in 1986, early severe corrosion of ECR began to be observed in the substructure of five major bridges (Group 1) built between 1978 and 1983 along US 1 in the Florida Keys<sup>1-3</sup>. The service ages for first observation of corrosion damage ranged from 6 to 12 years. The substructure of those bridges was built with permeable concrete of high

Copyright

©2009 by NACE International. Requests for permission to publish this manuscript in any form, in part or in whole must be in writing to NACE International, Copyright Division, 1440 South creek Drive, Houston, Texas 777084. The material presented and the views expressed in this paper are solely those of the author(s) and are not necessarily endorsed by the Association. Printed in the U.S.A.

Government work published by NACE International with permission of the author(s). The material presented and the views expressed in this paper are solely those of the author(s) and are not necessarily endorsed by the Association. Printed in the U.S.A.

apparent chloride diffusivity (e.g.  $D_{app} \sim 10^{-7} \text{ cm}^2/\text{s}$ ). Other Florida ECR marine bridges built during the same period and having  $D_{app}$  values approaching those of Group 1 were projected to show corrosion damage starting on the following decade or two<sup>4</sup>. Recent examination of four or those bridges (Group 2) confirmed that projection in each case<sup>5-6</sup>. Other recently examined Florida ECR bridges (Group 3) were built with very low permeability concrete having correspondingly low  $D_{app}$  values (e.g.  $D_{app} \sim 10^{-9} \text{ cm}^2/\text{s}$ ) at normally sound concrete locations. Those bridges were projected not to show early corrosion at normal locations<sup>4</sup> and that projection has also been confirmed by recent examinations. However, some incidence of local concrete deficiencies such as thin structural cracks always affects a small fraction of the substructure. Chloride transport through those deficiencies is much faster than through the matrix in otherwise low permeability concrete<sup>7</sup> and there is strong interest in establishing whether early corrosion can develop there. Recent work has confirmed such occurrence in at least one of those bridges<sup>6</sup>. This paper updates the history of development of damage in Florida ECR bridges during the first 3 decades of service in the light of current findings from Group 2 and Group 3 bridges, and examines the extent to which previous corrosion projections have been validated. Furthermore, the stage is set for more detailed modeling of future corrosion progression.

Table 1 lists the structures initially affected as well as additional bridges recently investigated, construction information, and the nomenclature used here. Three of the bridges (7MI, NIL and INK) were built with drilled shafts supporting columns with connecting struts. The LOK bridge has capped drilled shafts joined by a strut, and V-Piers rested on synthetic rubber pads placed on the caps. The CH5 bridge has drilled shafts with spread footers and precast, posttensioned box columns. The CH2, VAC, and SNK bridges have capped drilled shafts supporting columns. The CHO bridge has reinforced concrete columns with connecting struts, supported by capped prestressed piles. The SSK substructure consists of reinforced concrete columns with footers and struts in the low approach spans and elliptical post-tensioned columns for the high approaches. The PER substructure consists of reinforced concrete piles for the low approach and reinforced concrete columns on footers for the main span. The HFB substructure consists of reinforced concrete columns on footers.

The concrete used in the substructure of Group 1 and 2 bridges was cast in place (CIP) and conforming to FDOT Class IV specifications at the time of construction. Those specifications established water-to cement ratio  $w/c < 0.41$ , cement content =  $388 \text{ kg/m}^3$ , and 28-day strength  $> 23.5 \text{ MPa}$ . The specified maximum chloride content (acid soluble test) for concrete in these structures was  $0.24 \text{ kg/m}^3$ . Group 3 bridges utilized advanced concrete mix designs that included pozzolanic cement replacement. Specifications for SSK included  $w/c < 0.41$ , cementitious content  $444 \text{ kg/m}^3$  including 20% Type F fly ash, and 28-day strength  $> 34.5 \text{ MPa}$  for non-mass concrete and  $w/c < 0.35$ , cementitious content  $388 \text{ kg/m}^3$  including 28.5% fly ash and 28-day strength  $> 34.5 \text{ MPa}$ . Specifications for the other two Group 3 bridges had lower cementitious content. HFB concrete mix specifications included  $w/c < 0.41$ , cementitious content  $388 \text{ kg/m}^3$  including 35% Type C fly ash, and 28-day strength  $> 34.5 \text{ MPa}$ .

The design rebar concrete cover for the substructure was 7.6 cm for Group 1 bridges and for CHO. Design cover for VAC, SNK, and CH2 was larger, 15.3 cm. Design cover for SSK, PER and HFB was 10.2 cm. Substantial deviations from design value were often observed, especially in Group 1 bridges with round columns when the rebar cage was not precisely centered. As a result, some portions of the concrete had very low cover.

The ECR had been manufactured and coated following versions of ASTM 775 and ECR placement guidelines existing at the time of construction<sup>1-2</sup>. In most instances those guidelines allowed a maximum of 2% unrepaired surface damage at rebar surface. Rebar sizes ranged from #3 (10 mm diameter) to # 8 (25 mm). Rebar tie wires, as revealed by direct examination, were bare steel.

Conventional patch repairs and corrosion control procedures were conducted at various times in selected bents (piers) of Group 1 bridges. The most notable protective procedure was installation starting in 1988 of sacrificial sprayed-zinc anodes<sup>8</sup> at LOK (38 bents by 1996 plus 30 bents by 1998), NIL (31 bents by 1996), and 7MI (148 bents by 1998). In some instances the anodes were supplemented by immersed bulk anodes<sup>8</sup>. Other procedures included patching with concrete incorporating corrosion inhibiting admixtures, bar coatings, and proprietary cementitious repair mortars.

Examination of the structures was conducted at various levels. A general visual examination, performed periodically, was made by an experienced crew traveling slowly by boat and examining the entire perimeter of each bent in the bridge. If evidence of concrete cracking or other distress was observed, the substructure element was tested by sounding with a hammer for evidence and extent of internal concrete delamination. An area of delaminated concrete thus detected is designated for the purposes of this paper as a concrete spall. A delaminated area which extended from an area found to be spalled in a previous inspection was designated as a progressive spall. On selected bents from 7MI, NIL, LOK, INK, CH5, and CH2 the delaminated concrete was removed to expose the ECR and directly determine the extent of corrosion. Concrete cores were also extracted at select locations at 7MI, NIL, LOK, INK, and CH5. In selected bents from the Group 2 and 3 bridges, concrete core samples with ECR reinforcement at cracked and sound locations close to the cracks were also extracted. Additional documentation of corrosion damage in CH2 was provided by FDOT. Chloride ion (acid soluble) concentration profile measurements were conducted on cores extracted from selected bents. For crack locations, the concrete sampled for chloride analysis was from a region ~10mm wide centered on the crack.

## **FIELD CORROSION OBSERVATIONS**

### **Damage Progression - External Manifestations**

Figure 2 summarizes the results of visual and sounding examinations performed between 1986 and 2007 for group 1 and 2 bridges, which exhibited external manifestations of corrosion damage. The number of new spalls or progressive spalls observed on a bridge at a given inspection date was recorded. That number was then added to those observed in the previous inspections of the same bridge. In the figure the cumulative spall count was normalized by the number of bridge bents (For VAC, SNK, and CHO, only the number of bridge bents with ECR in marine service were counted). Spalls that occurred in regions formerly repaired (either by conventional patching or otherwise) were considered new spalls. For VAC and SNK, the areas where severe corrosion was observed at cracked concrete locations were considered as spalls even though concrete separation by hammer sounding could not be verified. This may be due to the large (~15 cm) concrete cover at these bridges. The damage functions are expressed in terms of spalls per bent to normalize for bridge size.

## Damage Characteristics

Group 1 Bridges. The following is a brief description of corrosion observations for this group; further details are found in Ref. 4. Typical spalls (Fig. 1) affected a projected area of  $\sim 0.3 \text{ m}^2$  on the surface of the concrete. Longitudinal cuts on the ECR surface with a sharp knife permitted easy peeling of the coating from the corroded regions, revealing extensive solid dark undercoating corrosion products typically magnetic and electronically conductive<sup>9</sup>. Occasionally, significant amounts of acidic liquid rich in chloride and iron were found as well<sup>10-11</sup>. Coating disbondment was also found on rebar locations adjacent and away from corroding regions. This disbondment without significant corrosion was found to be widespread in ECR after it was in service for a few years in Florida marine substructure conditions of all this and the other groups, even in the absence of chloride contamination of the concrete next to the rebar<sup>4,12</sup>. Examination of the underside of coatings from numerous ECR samples from all bridge groups, did not reveal any correlation between this disbondment and the usual forms of surface contamination expected in the coating process<sup>4,12</sup>. Chloride ion profiles indicated that extensive chloride penetration of the concrete had taken place in the splash zone of Group 1 structures (e.g., in the order of  $4 \text{ kg/m}^3$  at rebar depths after only 2 yrs). Apparent chloride diffusion coefficients ( $D_{\text{app}}$ ) determined from the chloride profiles for the splash zone ranged from  $\sim 10^{-8} \text{ cm}^2/\text{sec}$  to as much as  $\sim 6 \times 10^{-7} \text{ cm}^2/\text{sec}$ <sup>4,13</sup>. These high diffusivities agreed with concrete resistivity readings as low as  $\sim 1 \text{ k}\Omega \text{ cm}$  in the tidal region<sup>4,14,15</sup>.

Group 2 Bridges. Corrosion evaluations at CH2 for the current investigation were cursory but those and records from FDOT routine surveys showed extensive corrosion damage not unlike that observed at the Group 1 bridges. Typical corrosion distress is characterized by extensive concrete cracking (as wide as 1.3 mm with spalled concrete (average  $\sim 2.9 \text{ m}^2$ ) typically in the splash area but with several instances extended to above and below it. As in the Group 1 bridges, the concrete in CH2 showed indications of high permeability. At 25 y age the chloride concentration at  $\sim 15 \text{ cm}$  reinforcement depth and elevations 0.3-2 m AHT was as much as  $6.5 \text{ kg/m}^3$ . Assuming a typical chloride surface concentration value<sup>7</sup>  $C_s \sim 20 \text{ kg/m}^3$ ,  $D_{\text{app}}$  was estimated to be in the order of  $\sim 10^{-7} \text{ cm}^2/\text{s}$ . Low concrete resistivity (3-30 kohm-cm) was measured as well at elevations 0.3-1.5 m AHT. Severe coating distress and disbondment was observed at spalled concrete locations. ECR in areas away from distressed concrete locations was not tested.

Details on the corrosion examination of ECR from VAC, SNK, and CHO can be found in refs. 5 and 6. Extensive ECR corrosion was observed in VAC and CHO and to a lesser extent on SNK. The ECR corrosion at these bridges was accompanied by concrete cracking. Cracks were as wide as 0.3, 0.08, and 1 mm at VAC, SNK, and CHO, respectively. The cracks at VAC and SNK were not noticed in surveys conducted a decade earlier, and in one instance at VAC there was associated deeper cracking closer to the rebar. Those characteristics suggest that the cracking in these bridges was the result of expansive corrosion products, but as the evidence is limited the existence of at least some preexisting cracking cannot be ruled out. Instances of wide cracks at CHO were accompanied by concrete spalling as large as  $0.42 \text{ m}^2$ . All examinations in these bridges showed significant coating disbondment at and away from distressed concrete locations. Apparent chloride ion diffusion coefficients ranged from  $10^{-8}$  to  $\sim 3 \times 10^{-7} \text{ cm}^2/\text{s}$ . In most cases chloride concentrations at reinforcement depth amply exceeded values that are commonly assumed to be the threshold ( $C_T$ ) for corrosion initiation of steel in concrete<sup>16</sup>. Any evidence of preferential chloride penetration through cracks was obscured due to the high chloride bulk diffusivity prevalent at the sea splash locations examined;

chloride penetration profiles were not well differentiated in cracked/ uncracked concrete core pairs<sup>5,6</sup>.

Group 3 Bridges. Detailed results from Group 3 bridges are given in references 5 and 6, and a summary follows.

In SSK and PER little to no corrosion was observed at any examined on-water locations despite the presence of pre-existing structural cracks as wide as ~0.3 mm and with well manifested enhanced chloride penetration there at SSK. At elevations exposed to sea splash, chloride ion concentration at reinforcement depth for cracked concrete was ~2 kg/m<sup>3</sup>, close to or exceeding typically assumed threshold values<sup>16</sup>. Larger cracks, some of which had been repaired earlier on by epoxy-injection showed efflorescence. Consistent with the expected low permeability for the concrete used in these bridges, very low diffusivities (in the order of 10<sup>-9</sup> cm<sup>2</sup>/s) were measured in sound concrete<sup>1,7,15</sup>. The surface resistivity of the concrete was correspondingly very high. No concrete delamination was observed or detected by hammer sounding on any cracked or sound sections. Coating spot knife tests indicated complete coating disbondment on the surface of the ECR exposed by coring both at on- or off-crack locations. Despite that disbondment, no evidence of significant corrosion was observed except for vestigial rust at or near small coating breaks damaged during or before construction. That rust did not appear to reflect ongoing corrosion. For on-crack cores no correlation was found between the presence or position of the crack and the extent or location of vestigial rusting or coating disbondment in the ECR segments.

In HFB, severe localized ECR corrosion at cracks in otherwise highly impermeable concrete in a Florida marine substructure was documented for the first time<sup>6</sup>. Vertical cracks were frequently observed on the concrete footers; several large cracks were as wide as 1.0 mm and sometimes propagated past reinforcement depth. The cracks had been documented in previous inspections and are likely due to differential curing in the bulk of the concrete. As in SSK, distinct preferential chloride penetration at cracks was observed in this bridge at elevations exposed to sea splash, and chloride ion concentration at the 10 cm reinforcement depth for cracked concrete was ~2 kg/m<sup>3</sup>, near or above typically assumed threshold values<sup>16</sup>. Much lower chloride levels were measured at bar depth in adjacent sound concrete, consistent with the low chloride bulk diffusivity (~7x10<sup>-9</sup> cm<sup>2</sup>/s) determined for this low permeability concrete. The bars extracted from corroding locations at HFB were examined in detail. Upon removal of the coating (which was found to be fully disbonded) the underlying surface was relatively dry, with dark corrosion product regions. Metallographic examination of the cross section of the bar at severe corrosion locations revealed that corrosion had proceeded in relatively uniform fashion within a region several mm wide to as much as ~1 mm deep. Except for some surface reddening, the corrosion products in that region were dense and dark-gray, suggesting a low oxidation state. The corrosion product-base metal interface was examined at higher magnification revealing upon etching a ferrite-pearlite grain structure that extended, with no indication of microstructural alteration, all the way up to the corrosion penetration front where it was being consumed. In addition to the severe localized corrosion, vestigial surface corrosion similar to that observed in SSK was also observed at several crack locations. No physical indication of corrosion was observed at any of the matching sound concrete locations. It is noted that at HFB concrete surface resistivity was very high (Mohm-cm range) even in the tidal zone. These unexpectedly high values are not likely due to concrete carbonation, since carbonated concrete depth was small (<1mm) as it is typically so in similar marine substructures<sup>13</sup>. The causes for the unusually high resistivity values are under investigation.

## DISCUSSION

### Corrosion Mechanism

A corrosion development scenario for ECR in the affected Florida marine concrete substructure was proposed in our earlier work<sup>3,4,12</sup> to explain the observed damage. The proposed sequence was generally in agreement with the results from the initial investigations. Findings from the more recent surveys further supported that scenario, which is reproduced here to reflect current understanding of the matter. Stages before and after the structure is placed in service are considered.

Pre-placement in service stage: ECR contained a small number of initial coating imperfections, as permitted by the acceptance criteria at the time. The bars were cut, shaped and then shipped and fabricated as required. Shipping introduced additional surface damage; fabrication mechanically introduced some disbondment<sup>3,4,9-12</sup>. The bars were then exposed to the construction yard environment for a time that may have ranged from days to over a year. Salt water (from sea spray) exposure at the yard created additional disbondment<sup>4</sup>; further deterioration might have resulted from heating/cooling cycles, ultraviolet exposure and additional mechanical damage during handling. Rebar cage assembly procedures, positioning in concrete forms, as well as concrete pouring and vibration, created additional surface damage.

In-service stage: The ECR was exposed to a low to intermediate chloride concrete environment for some time depending on the rate of chloride penetration. During that time the concrete pore solution interacted with the rebar coating, and penetrated between coating and metal in regions where disbondment had taken place during pre-service and aggravated coating disbondment<sup>12</sup>. Upon reaching a critical threshold chloride concentration, corrosion began at the metal exposed at imperfections, and in the crevices which exist below disbonded coating. Corrosion macrocells developed with cathodic regions in regions of good oxygen availability. Cathodic action took place not only at exposed metal at imperfections but also to some extent into the surrounding disbonded crevices. Low concrete resistivity and a measure of electrical continuity of the rebar cage (at accidental contact points) promoted longer range macrocell action<sup>11</sup>, making for an unfavorable anode-to-cathode ratio. The resulting intense action at the anodic portion caused additional disbondment and corrosion at the crevices. Eventually, the corrosion morphology consisted of extensive coating delamination, accumulation of corrosion products and low pH liquid below the coating, and metal consumption manifested by spots of severe pitting on a background of more general wastage<sup>10</sup>. Externally observable corrosion developed then in a relatively short time, comparable to that experienced by plain rebar in a similar concrete environment.

In summary, the corrosion may be viewed as resulting from the presence of allowable (per specifications prevalent at the time of manufacturing) production imperfections which were then aggravated by fabrication, handling, and a severe construction yard environment. This was followed by placing the rebars in moist, warm, eventually high chloride-level substructure service which was conducive to severe corrosion, aggravated by extended macrocell formation. Additional insight on the corrosion mechanism of ECR in marine environment has been noted elsewhere<sup>17</sup>.

## Corrosion Progression

The damage function trends shown in Figure 2 provide important insight on the extent of the corrosion and its future development. For Group 1 Bridges the corrosion damage into the 3rd decade of service is conspicuous, with multiple spalls per pier on average. That damage affects a significant fraction of the area of the splash zone of each bridge, where the concrete surface area on the splash zone of a typical bent is  $\sim 20 \text{ m}^2$  and a typical spall affects  $\sim 0.3 \text{ m}^2$ . Damage is likely to have been worse without the application of protective anodes. Except for an offset toward shorter times for NIL, the functions are remarkably similar to each other. The damage at present appears to increase approximately linearly with time. If those trends were to continue, the total extent of damage would roughly more than double over the next 20-30 years of service. As repairs in marine substructure are very costly, corrosion would place a continuing and heavy repair and maintenance burden during the remaining service life of these structures.

In Group 2 Bridges, corrosion propagation at CH2 started the earliest and appeared to increase roughly linearly with time similar to Group 1 bridges. Damage in the other Group 2 bridges appeared to have started after  $\sim 25$  years in marine service. Corrosion deterioration was evident in CHO where spalled areas could easily be detected. Damage at VAC and SNK was not as conspicuous, and the origin of concrete cracking at corroded bar locations there could not be established as resulting exclusively from expansive corrosion products. The corrosion propagation trends at VAC and SNK may be anticipated to be similar to those at CH2 and the Group 1 bridges, but future confirmation is needed. In any event, the observation of significant ECR corrosion in the Group 2 Bridges verifies earlier damage projections for ECR structures in the Florida inventory having concrete with high  $D_{app}$  values<sup>4</sup>.

For the Group 3 Bridges, no concrete delamination or spalling was observed at any of the structures examined, but significant ECR corrosion was observed at cracked concrete locations of HFB. This latter observation is an important warning of potentially severe local damage in the future, so frequent monitoring of these and similar locations are advisable. Due to the otherwise high quality concrete and large concrete cover, early corrosion damage is not anticipated for sound concrete locations. However, there was widespread disbondment of the epoxy coating in all these structures even in sound concrete locations. This disbondment together with the observed frequent coating breaks is expected to facilitate corrosion initiation as chloride levels at the rebar depth increase in future decades.

## Performance Projections

To better understand the factors responsible for corrosion development and anticipate future needs for maintenance and repair, an effort was conducted to obtain quantitative damage projections. A statistical model to project performance of marine bridge substructure containing ECR was successfully applied in previous interpretations of the damage progression data<sup>18</sup>. Application to the current expanded data set is presented here. Briefly, the model divides the substructure surface into discrete elements, each experiencing damage evolution with a corrosion initiation stage (of duration  $t_i$ ) and a propagation stage of duration  $t_p$ <sup>14,19</sup> at the end of which the element is declared damaged. Each element is assumed to have its own value of surface chloride concentration  $C_s$ , concrete cover  $x$ ,  $D_{app}$ , threshold concentration  $C_T$ . Those parameters together establish the local value of  $t_i$  by assuming for simplicity a one-dimensional diffusion geometry<sup>18</sup>. The value of  $t_p$  for each element is

determined by assuming that the element has its own effective corrosion rate  $R$  resulting in corrosion penetration  $P$  that increases linearly with  $t-t_i$ , where  $t$  is time. There is growing evidence that cracking/spalling takes place when  $P$  reaches a given value  $P_{CRIT}$  which for macroscopically uniform corrosion is proportional to the ratio  $x/\Phi$ , where  $\Phi$  is the rebar diameter<sup>20</sup>. Rebar size varies relatively little over the structural elements of interest (mostly near size #6 (diameter ~20mm) so by treating  $\Phi$  as constant  $t_p$  may be approximated for modeling purposes<sup>21</sup> as  $t_p = kx$ , where  $k$  is proportional to  $R^{-1}$ .  $R$  is strongly influenced by the condition of the coating<sup>22,23</sup> such that ECR with substantial coating distress should corrode faster than in the absence of imperfections. Thus  $k$  is treated as a distributed model parameter that becomes smaller as the extent of ECR coating distress increases.

The values of  $C_s$ ,  $D_{app}$  and  $x$  were assumed to have average values and element-to-element variability consistent with field observations in these structures. The variabilities were treated as stemming from normal distributions truncated as indicated below<sup>18</sup>. A fixed value of  $C_T$  was assumed for simplicity. Laboratory observations suggest that under simple conditions  $C_T$  for ECR is on the order of the value for plain steel bar<sup>4</sup>, which may in turn be estimated as being proportional to the cement content (CF) of the concrete,  $C_T \sim 0.004CF$ .<sup>16</sup> The parameter  $k$  was assigned variability but implemented only stepwise over 3 different finite levels, plus another level designating elements with essentially unblemished rebar coating. The fraction of elements having each of the coating distress levels (or lack thereof) was also a model input.

Damage projections were made by applying the above parameter distributions to a large population of elements, and tallying the fraction of elements reaching  $t_i+t_p$  for increasing time intervals<sup>18</sup>. Each element was assigned the same surface area value, equal to that of a typical spall, and the total number of elements corresponded to a multiple of the typical portion of a bent exposed to aggressive conditions. Thus the fraction of cracked/spalled elements at a given time was equal to the number of spalls per bent, allowing direct comparison to the field data.

Cases modeled corresponded to the Group 1 Bridges, and two subsets of the Group 2 bridges. Differentiation between cases applies only to  $x$  and  $D_{app}$  values. All calculations assumed initially chloride-free concrete.

Table 2 lists the values selected for model input for each case. The exposed bent area  $A_f$  and element area  $A_e$  are based on typical prevalent structure and spall dimensions. The value of  $C_T$  reflects a representative value of CF (388 kg/m<sup>3</sup>) consistent with those noted earlier. The average  $C_s$ ,  $x$  and  $D_{app}$  values and their standard deviations are representative of those encountered in the affected bridges<sup>4</sup>. It is recognized that as those magnitudes cannot assume negative values, the actual distributions must depart from simple Gaussian shape. However, as more precise information on distribution character is not available, truncated normal distributions are used instead as a compromise. Thus all distributions are truncated at zero, and  $C_s$  is furthermore truncated at 25 kg/m<sup>3</sup> which is representative of a salt-saturated pore water condition<sup>7</sup>. The severe exposure regime and high concrete permeability conditions in Group 1 (reflected in the high average  $C_s$  and  $D_{app}$  values) result in exceeding the threshold concentration at the rebar depth very early (e.g one year or so) in the life of the structure even for average cover locations. Consequently, for Group 1 the corrosion development is expected to be dominated by the propagation stage (the value of  $t_p$ ), and less sensitive to the parameters that affect only  $t_i$ <sup>7</sup>.

The projected value of  $t_p$  does depend strongly on  $x$  and  $k$  values. The first is measured directly, but the  $k$  distribution can only be inferred. Toward representing closely the observed damage progression, the assignment of  $k$  values over the rebar assembly was made by assuming that only a small fraction (2%) of the rebar assembly was responsible for the earliest observations of damage. That fraction had a low value of  $k = 0.14$  y/mm, which results in  $t_p = 7$  years when  $x = 50$  mm. As  $t_i$  is very short, that fraction was consequently responsible for the very first failures projected. Increasingly large fractions of the assembly were assumed to have correspondingly less distress and larger propagation times. This approach reflects the expectation that rebar segments with a high incidence of coating distress are likely to have the highest corrosion rates and therefore the shortest  $t_p$  values. The chosen distribution for  $k$  then effectively states that there was a small fraction of the rebar with severe coating distress, and proportionally less distress on increasingly larger fractions of the assembly.

Resulting projections for each of the cases (thick solid line) are shown in Figures 3-4. The corresponding actual damage functions from Figure 2 are reproduced for each pertinent case. The model projection for Group 1 bridges (Figure 3) reasonably reproduced the duration of the initial period where damage was minimal, and the subsequent steady rise. The present choice of input parameters replicates that used in Ref 18, which was based on fitting to data that terminated at earlier times for two of the bridges (NIL and LOK), but the overall match continues to be similarly adequate for the newer data as well. Sensitivity tests confirmed that the damage projection was only modestly influenced by changes in the distribution of  $D_{app}$  or  $C_s$ , or by variations in  $C_T$ , in agreement with the basis for the choice of model parameters indicated above. Additional calculations with alternative  $k$  distributions indicated also that reasonable fit to observed behavior could be obtained only if the percentage of the assembly assigned low  $k$  values (yielding  $t_p$  values of only a few years) was quite small.

The dashed lines in Figures 3-4 represent the separate contribution to the total damage of each of the finite assumed distress fractions; addition of which corresponds to the thick solid line. As shown in figures 3, as time progresses the projected damage increase results from fractions with increasingly greater  $k$ . Whether future damage will continue along the present trend depends, in this scheme, on the extent of coating distress on the rest of the rebar assembly. If the remaining rebar coating were in very good condition, damage would continue for some time at the present nearly constant rate and then saturate at some intermediate level. The present choice of  $k$  distribution assigns finite values to only the first 14% of the rebar assembly, so projected damage saturation would take place at  $\sim 9$  spalls per bent. At present the highest recorded value (for NIL, evaluated in 2005) reaches 4.3 spalls per bent without signs of slowing down, but the available data cannot preclude development of saturation in the relatively near future. Conversely, if the surface condition of the remaining rebar were poor or marginal, damage progression could easily continue to reach increasingly higher levels.

Data for the Group 2 bridges are too limited for detailed evaluation, but the model projections are in the order of the observed deterioration. Both subsets projected later damage development than for Group 1. The subset VAC, SNK, and CH2 (VSC on Table 2) had values of  $D_{app}$  that were comparable to each other but not much smaller than those for Group 1. However, the average rebar cover of subset VSC was twice as high as for Group 1. Under the model ruling equations<sup>18</sup> doubling the cover resulted in a fourfold increase in  $t_i$ , and in doubling the value of  $t_p$  which shifted the development of damage accordingly. The actual

damage evolution in CH2 is somewhat faster than its projected value, but that difference partially stems from imprecise information on the range of  $D_{app}$  for that bridge as only a cursory examination performed there. CHO was placed into another subset (C on Table 2) as its average  $D_{app}$  was notably smaller than for the other bridges. That difference resulted in a significant increase of projected  $t_i$ , toward increasing initiation stage control of the deterioration. Thus, CHO had longer projected times to damage than in the first Group 2 subset, even though the average cover value was less than for that first subset.

The interpretation and model described above involve numerous assumptions and simplifications. One such simplification includes assuming simple Fickian diffusion with time and depth independent  $D_{app}$  with constant surface concentration  $C_s$ .<sup>18</sup> Notable among the many issues not addressed are alternative  $C_T$  regimes as reported elsewhere<sup>13</sup>, including possible higher  $C_T$  due to coupling with nearby anodic regions<sup>24</sup> which could substantially alter the damage projection. This latter factor is examined in detail in a companion paper of these proceedings<sup>25</sup>. Future model improvements should resolve some of these issues. The present projections nevertheless serve to provide insight on the key factors responsible for the observed damage and in formulating corrosion management strategies.

### **Overall considerations and behavior in locally deficient concrete**

The field observations and insight from the above modeling projections indicate that ECR corrosion in the Florida bridges resulted from a combination of factors. Those include a highly aggressive service environment which, in the absence of a thick cover of highly impermeable concrete, rapidly left the epoxy film as the only remaining corrosion protecting barrier on the steel bar. Given also the inherent vulnerability of the film to flaws and disbondment from the base metal, corrosion quickly ensued with electrochemical aggravating factors noted earlier. As the modeling arguments showed, significant corrosion of even a relatively small fraction of the rebar assembly could manifest itself as extensive and conspicuous damage, which can continue increasing for many years.

As shown by the absence of external signs of damage in the Group 3 bridges, no severe ECR corrosion developed when the coated bar was protected by a thick cover of sound, very low permeability concrete with  $D_{app}$  values nearly two orders of magnitude lower than those in Group 1. Significant amounts of coating flaws existed in those cases too, as well as widespread loss of adhesion between coating and base metal, so corrosion is expected to ensue once the chloride content at the rebar exceeds an effective threshold level. However, such event would likely be many decades into the future given the very slow chloride penetration. It is cautioned that part of the inventory of ECR Florida bridges has substructure with intermediate  $D_{app}$  values not unlike those in CHO<sup>4</sup>. In those bridges corrosion may well begin to develop in the relatively near future, albeit per experience from the Group 2 bridges and per model projections, at a more moderate rate of increase than that seen in Group 1.

As noted above and from findings in related investigations<sup>4-6</sup> the protection of a thick cover of low permeability concrete can be seriously diminished locally in the presence of cracks, lift lines or other local deficiencies. Corrosion may not only develop locally as noted in HFB, but the strong deterioration seen there may reflect also adverse galvanic coupling with nearby passive steel at other coating break locations<sup>26,27</sup>. Such effect could lead to severe local reduction of cross section and associated risk of reinforcement failure<sup>28</sup>. The consequences of that form of deterioration may be mitigated in part by the relatively small

incidence of cracking<sup>7</sup> when viewed in terms of number of cracks per length of waterline perimeter, thus representing a limited number of spots with likely incidence of damage. In addition to the continuing monitoring of these locations recommended above, expansion of predictive models to cover this form of damage and quantify its effects should be conducted as well.

## **CONCLUSIONS**

1. Damage from corrosion of ECR has continued to develop steadily in the substructure of five major Florida Keys bridges. Since the first indications of corrosion ~6 y after construction, damage increased at a rate of ~0.1 spall per bent per year until the present ~25 y age of the structures, with no indication of slowdown. Externally recognizable ECR corrosion damage began to be noticeable at four other Florida bridges ~2 decades after construction and continuing into the 3rd decade.
2. Early corrosion in the Florida bridges resulted from a combination of factors, including a highly aggressive service environment which, in the absence of a thick cover of highly impermeable concrete, rapidly left the epoxy film as the only remaining corrosion protecting barrier on the steel bar. Given also the inherent vulnerability of the film to flaws and disbondment from the base metal, corrosion quickly ensued with electrochemical aggravating factors such as the formation of extended macrocells.
3. Experimental results and predictive model calculations indicate that the propagation stage of corrosion dominated damage development in the structures that showed early deterioration. Significant corrosion of even a relatively small fraction of the rebar assembly could manifest itself as extensive and conspicuous damage, which can continue increasing for many years.
4. No severe ECR corrosion developed in situations where the coated bar was protected by a thick cover of sound, very low permeability concrete. However, there was widespread disbondment of the epoxy coating in all these structures even in sound concrete locations. This disbondment together with the observed frequent coating breaks are expected to facilitate corrosion initiation as chloride levels at the rebar depth increase in future decades.
5. Significant ECR corrosion was observed at previously cracked concrete locations of one of the bridges built with otherwise very low permeability concrete. This observation is an important warning of potentially severe local damage in the future. Frequent monitoring of these and similar locations is advisable, as is the development of predictive models for corrosion of ECR in locally deficient concrete.

## **ACKNOWLEDGMENTS**

This work was supported by the Florida Department of Transportation (FDOT). The findings and conclusions expressed here are those of the authors and not necessarily those of the FDOT. The assistance with field inspections of many collaborators at the FDOT State Materials Office and from Concorr Florida, Inc. is greatly acknowledged, as is that of numerous student participants in the University of South Florida College of Engineering Research Experience for Undergraduates program.

## REFERENCES

1. Kessler, R. and Powers, R. Interim Report, Corrosion Evaluation of Substructure, Long Key Bridge, Corrosion Report No. 87-9A, Materials Office, Florida Department of Transportation, Gainesville, 1987.
2. Powers, R. Corrosion of Epoxy Coated Rebar, Keys Segmental Bridges, Corrosion Report No. 88-8A, Florida Dept. of Transportation, Gainesville, Florida, 1987.
3. Sagüés, A., Powers, R. and Kessler, R., "Corrosion Processes and Field Performance of Epoxy Coated Reinforcing Steel in Marine Substructures", Paper No. 299, Corrosion/94, NACE International, Houston, 1994.
4. Sagüés, A. "Corrosion of Epoxy-Coated Rebar in Florida Bridges", Final Report to Florida DOT, WPI No. 0510603, Florida Department of Transportation, Tallahassee, FL, May, 1994.
5. Lau, K., Sagüés, A.A., and Powers, R.G. Corrosion/2007, Paper No.07306, NACE International, Houston, TX, 2007.
6. Lau, K., Sagüés, A.A., and Powers, R.G. Corrosion/2008, Paper No.08311, NACE International, Houston, TX, 2008.
7. Sagüés, A.A. et al, "Corrosion Forecasting for 75-Year Durability Design of Reinforced Concrete," Final Report to Florida D.O.T. WPI 0510805. Dec. 2001, Available online, [www.dot.state.fl.us](http://www.dot.state.fl.us).
8. Kessler, R. and Powers, R., "Zinc Metallizing for Galvanic Cathodic Protection of Steel reinforced Concrete in a Marine Environment", Paper No. 324, Corrosion/90, NACE International, Houston, 1990.
9. Sagüés, A., Powers, R., Zayed, A., "Marine Environment Corrosion of Epoxy-Coated Reinforcing Steel", in Corrosion of Reinforcement in Concrete, C. Page, K.Treadaway and P. Bamforth, Eds., pp.539-549, Elsevier Appl. Sci., London-New York, 1990.
10. Sagüés, A. and Powers, R., "Effect of Concrete Environment on the Corrosion Performance of Epoxy-Coated Reinforcing Steel", Paper No. 311, Corrosion/90, NACE International, Houston, 1990.
11. Sagüés, A. , Perez-Duran. H. and Powers, R., Corrosion, Vol 47, p.884, 1991.
12. Sagüés, A. and Powers, R. "Coating Disbondment in Epoxy-Coated Reinforcing Steel in Concrete - Field Observations", Paper No. 325, Corrosion/96, NACE International, Houston, 1996.
13. Hartt, W., Lee, S.K. and Costa, J., "Condition Assessment and Deterioration Rate Projection for Chloride Contaminated Concrete Structures" p.82 in Repair and Rehabilitation of Reinforced Concrete Structures: The State of the Art, W.P. Silva-Araya, O. T. de Rincon and L. Pumarada O'Neill, Eds., ASCE, Reston, VA, 1998.

14. Berke, N.S. and Hicks, M.C., "Estimating the Life Cycle of Reinforced Concrete Decks and Marine Piles using Laboratory Diffusion and Corrosion Data", p. 207 in Corrosion Forms and Control for Infrastructure, ASTM STP 1137, Victor Chaker, Ed., ASTM, Philadelphia, 1992.
15. Andrade, C., Alonso, C. and Goni, S., "Possibilities for Electrical Resistivity to Universally Characterise Mass Transport Processes in Concrete", p.1639, in Concrete 2000, Vol 2., R.K. Dhir and M.R. Jones, Eds., E. & F.N. Spon, London, 1993.
16. Bentur, A., Diamond, S. and Berke, N., Steel Corrosion in Concrete, E&FN Spon, New York, 1997.
17. Nguyen, T. and Martin, J.W. JCT Research, Vol.1, no.2, pp.81-92, 2004.
18. Sagüés, A.A. Corrosion. 59, 10 (2003): p.854-866
19. Tuutti, K., Corrosion of Steel in Concrete, Swedish Cem. and Conc. Res. Inst, 1982.
20. Torres-Acosta, A., Sagüés, A.A., ACI Mater. J. 101, 6 (2004): p. 501-507.
21. "Concrete Cover Cracking with Localized Corrosion of the Reinforcing Steel", A.A. Torres-Acosta and A.A. Sagüés, p. 591 in Proc. of the Fifth CANMET/ACI Int. Conf. on Durability of Concrete, SP-192, V.M Malhotra, Ed., American Concrete Institute, Farmington Hills, Mich., U.S.A., 2000.
22. Clear, K.C., "Effectiveness of Epoxy-Coated Reinforcing Steel", Concrete International, p. 58, Vol. 14, May 1992.
23. McDonald, D.B, Pfeifer, D.W. and Sherman, M.R, "Corrosion Evaluation of Epoxy-Coated, Metallic-Clad and Solid Metallic Reinforcing Bars in Concrete", Report No. FHWA-RD-98-153, Nat. Tech. Info. Service, Springfield, VA, 1998.
24. Sagüés, A.A. and Kranc, S.C. "Model for a Quantitative Corrosion Damage Function for Reinforced Concrete Marine Substructure" in Rehabilitation of Corrosion Damaged Infrastructure, p.268, Proceedings, Symposium 3, 3rd. NACE Latin-American Region Corrosion Congress, P.Castro, O.Troconis and C. Andrade, Eds., ISBN 970-92095-0-7, NACE International, Houston, 1998.
25. Sagues, A.A., K. Lau, and S.C. Kranc. "Modeling of Corrosion of Steel in Concrete with Potential-Dependent Chloride Threshold." 17<sup>th</sup> Int. Corr. Conference. No. 4006. NACE Int. Houston, TX. 2008.
26. Kranc, S.C. and A.A. Sagüés "Computation of Corrosion Distribution Of Reinforcing Steel in Cracked Concrete", in Proc. International Conference on Corrosion and Rehabilitation of Reinforced Concrete Structures, Orlando, FL, Dec. 7-11, 1998, CD ROM Publication No. FHWA-SA-99-014, Federal Highway Administration, 1998.
27. Raupach, M. Construction and Building Materials, Vol. 10, p. 329, 1996.
28. Tinnea, J. "Localized Corrosion Failure of Steel Reinforcement in Concrete Field Examples of the Problem." 15<sup>th</sup> Int. Corr. Conference. Paper 706. NACE Int. Houston, TX. 2002.

Table 1 ECR Bridges

	Bridge Name		Year Built	Average D (cm <sup>2</sup> /s)	$\rho$ (k $\Omega$ -cm)	cement factor (kg/m <sup>3</sup> )	fly ash	Widest crack width (mm)	ECR Clear Cover (cm)
Group 1	Seven Mile	7MI	1982	$2 \times 10^{-7}$	5-24	388	no	>1 <sup>†</sup>	7.6
	Niles Channel	NIL	1980	$2 \times 10^{-7}$	-			>1 <sup>†</sup>	
	Indian Key	INK	1981	$\sim 10^{-7}$	-			>1 <sup>†</sup>	
	Channel 5	CH5	1982	$\sim 10^{-7}$	-			>1 <sup>†</sup>	
	Long Key	LOK	1982	$2.9 \times 10^{-7}$	-			>1 <sup>†</sup>	
Group 2	Channel 2	CH2	1981	$\sim 10^{-7}$	0.4-12	388	no	>1 <sup>†</sup>	15.3
	Vaca Cut	VAC	1982	$2.6 \times 10^{-7}$	4-50			0.28	15.3
	Snake Creek	SNK	1981	$9.0 \times 10^{-8}$	4-40			0.08	15.3
	William Marler	CHO	1979	$1.8 \times 10^{-8}$	16-128			>1 <sup>†</sup>	7.6
Group 3	Sunshine Skyway	SSK	1986	$1.1 \times 10^{-9}$	150	445	20% Type F	0.64	10.2
	Lillian	PER	1981	$3.1 \times 10^{-9}$	113-275	-	Yes	0.25	
	Howard Frankland	HFB	1991	$7.3 \times 10^{-9}$	high M $\Omega$ -cm	388	35% Type C	>1	

† Spalled Concrete

Table 2. Model Input Parameters

		Group 1	Group 2
			(VSC) (C)
Af	Surface area of bent exposed to severe corrosion		20 m <sup>2</sup>
Ae	Typical spall area		0.3 m <sup>2</sup>
C <sub>T</sub>	ECR chloride concentration threshold		1.55 kg/m <sup>3</sup>
$\mu$ Cs	Average surface chloride concentration		12 kg/m <sup>3</sup>
$\sigma$ Cs	Standard deviation of surface chloride concen.		Cs/4
Cs <sub>max</sub>	Maximum surface chloride concentration		25 kg/m <sup>3</sup>
$\mu$ x	Average rebar cover	76 mm	148 mm 87 mm
$\sigma$ x	Standard deviation of rebar cover		x/4
$\mu$ D <sub>app</sub>	Average chloride diffusion coefficient	$2 \times 10^{-11}$ m <sup>2</sup> /s	$1.7 \times 10^{-11}$ m <sup>2</sup> /s $1.3 \times 10^{-12}$ m <sup>2</sup> /s
$\sigma$ D <sub>app</sub>	Standard deviation of diff. coeff.		D/4
k'	Proportionality constant for propagation time (Percentages indicate fraction of the surface assigned to the value)		0.14 y/mm (2%) 0.28 y/mm (4%) 0.56 y/mm (8%)

Note: Cs, x and D<sub>app</sub> were assumed to be distributed as in an standard deviation, but truncated by zero and as shown by Cs<sub>max</sub>, and normalized accordingly.



Figure 1. Typical Spall Appearance (7MI)

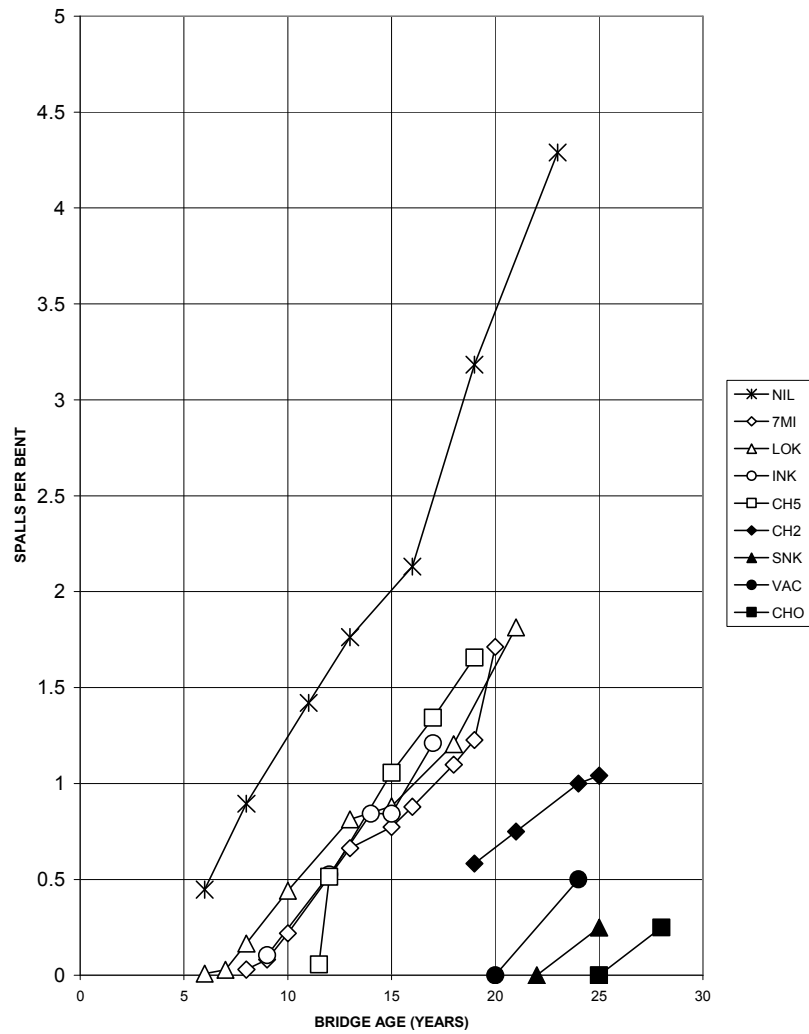


Figure 2. Progression of corrosion as function of time.

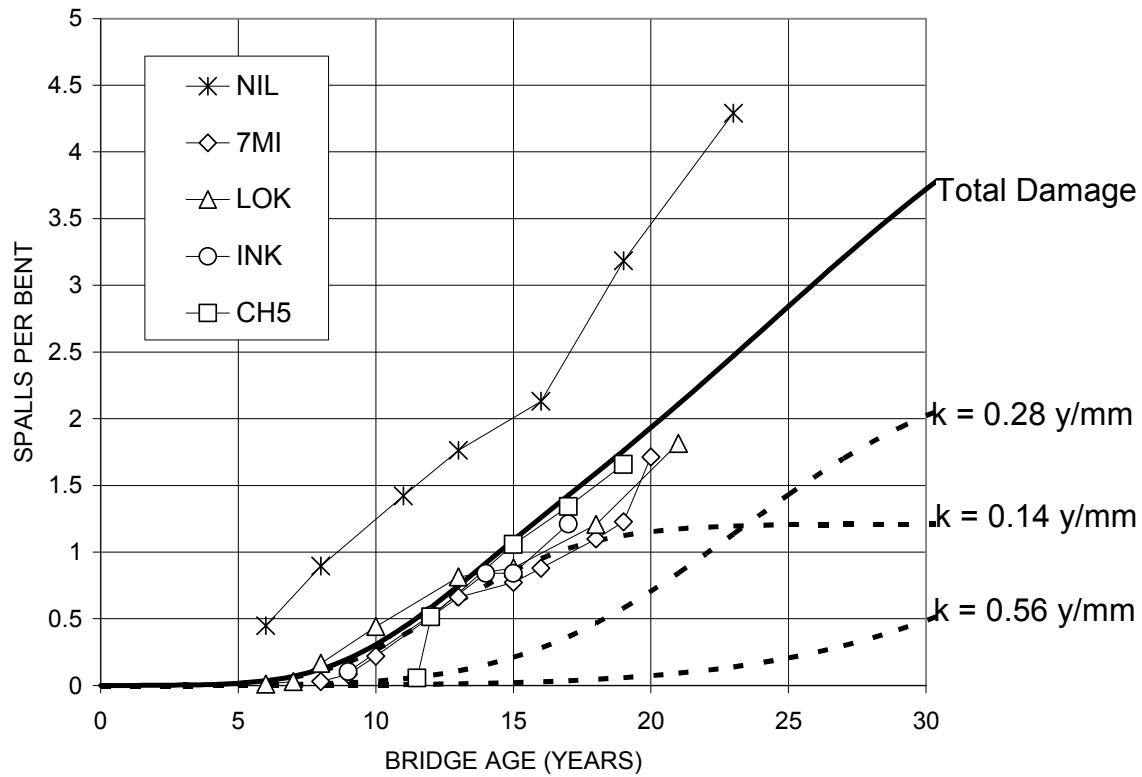


Figure 3. - Projected damage function for Group 1 bridges. Thick bold line: total damage projection. Dashed lines: partial damage from each of the rebar assembly fractions considered: 2% of the rebar with  $k=0.14 \text{ y/mm}$ ; 4% with  $k=0.28 \text{ y/mm}$  and 8% with  $k=0.56 \text{ y/mm}$ .

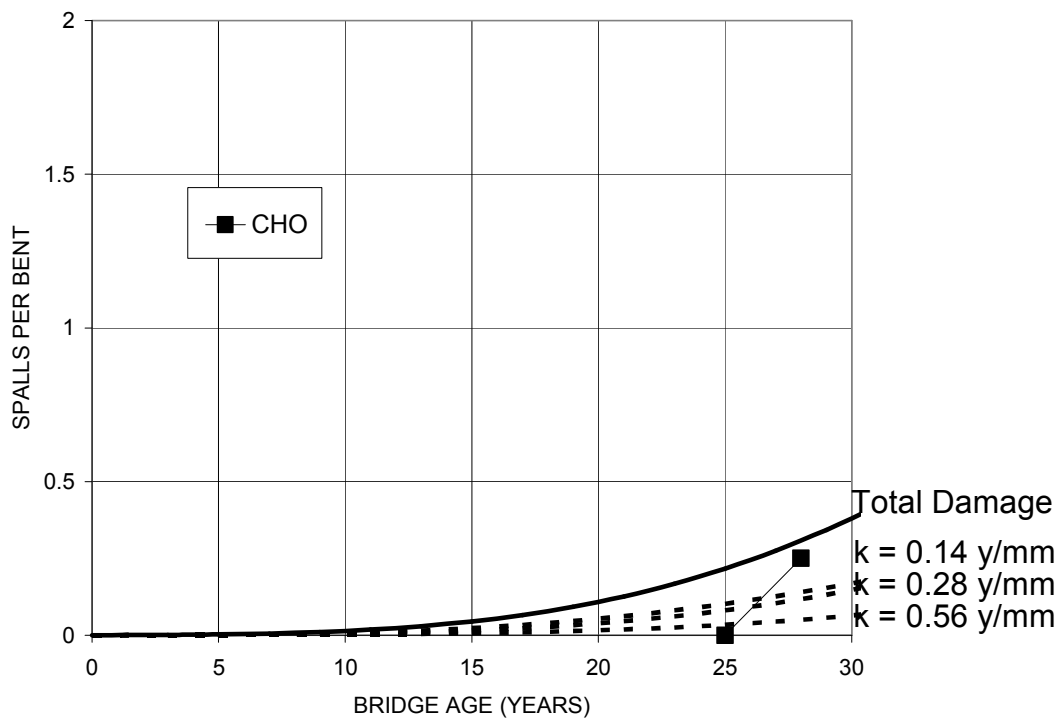
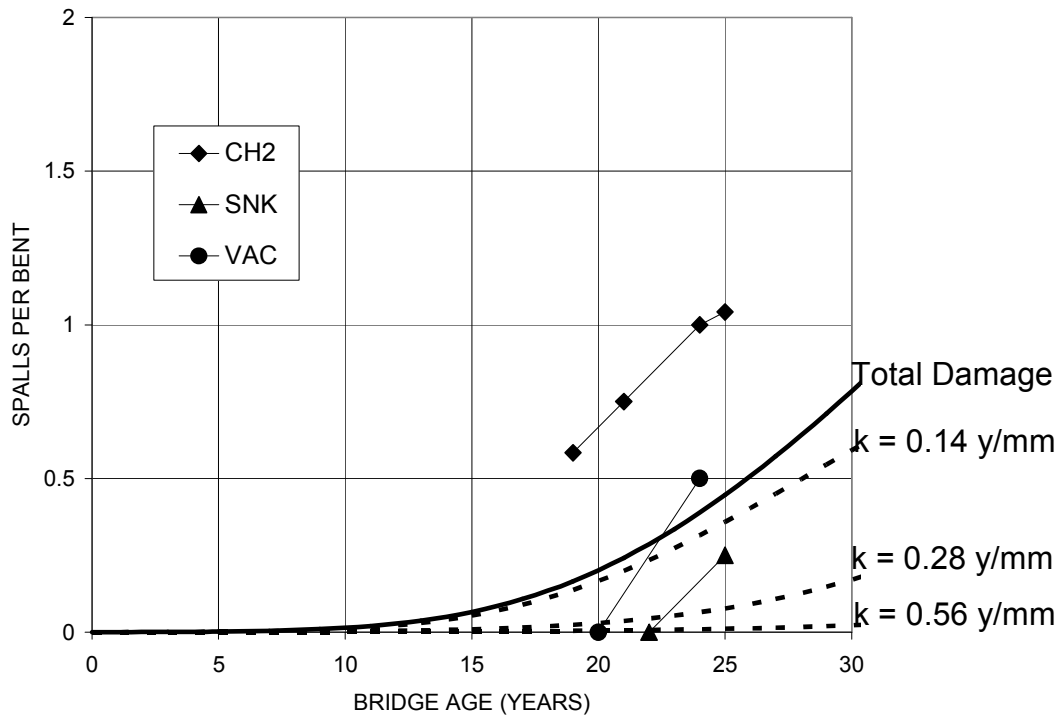


Figure 4. Projected damage function for Group 2 bridges. Thick bold line: total damage projection. Dashed lines: partial damage from each of the rebar assembly fractions considered; 2% of the rebar with  $k=0.14$  y/mm; 4% with  $k=0.28$  y/mm and 8% with  $k=0.56$  y/mm.